Non-linear Stability Boundary Assessment of Offshore Wind Power Plants Under Large Grid Disturbances

Sujay Ghosh*, Mohammad Kazem Bakhshizadeh†, Guangya Yang*, Łukasz Kocewiak† and Bikash Pal‡
*Technical University of Denmark, Anker Engelunds Vej 1, 2800, Denmark.
Email: sujgh@dtu.dk
†Ørsted Wind Power, Nesa Allé 1, 2820, Denmark.
‡Imperial College London, London SW7 2BX, United Kingdom

***Abstract*—Recent research has identified that the dynamics of the phase-locked loop (PLL) converter control contributes to grid-synchronisation instability when a wind turbine (WT) system is perturbed with large disturbances (i.e. severe grid faults). The metric for such stability assessment is the region of attraction (ROA), which signifies a subset of the system's state-space in which all the trajectories converge to a stable equilibrium point. This paper reviews the performance of transient stability assessment methods such as the time-domain methods, i.e. time-domain simulations, and phase portrait analysis; and the analytical methods, i.e. equal-area criteria, and Lyapunov's direct method, for estimating the ROA of a post-disturbance WT system. Additionally, some highlights of advanced methods for transient stability assessment, such as the sum-of-squares optimisation technique and machine learning methods, are also presented. The time-domain and analytical methods are applied on an equivalent swing equation model of a WT, where it is seen that the time-domain methods are less complex and provides accurate ROA, accompanied by a high computation burden. On the other hand, the analytical methods are complex and provides either slightly optimistic or highly conservative estimates of the ROA; however, such methods are very fast due to closed-form solutions.**

I. Introduction

With the rapid development in renewable energy technologies, the power generation share from converter-interfaced offshore wind power plants (WPPs) is expected to increase considerably, which is likely to introduce challenges in the stability control of future power grids. In this regard, some system operators have started to impose strict grid code requirements, aiming to operate the WPPs like a conventional power plant [1]-[3]. The converter-interfaced WPPs exhibit fast and complex transient behaviour under grid disturbances [4]-[5]; in the case with grid-following controls, this complex behaviour is mainly driven by the dynamics of the phase-locked loop (PLL), which must maintain synchronism even under large disturbances (i.e. severe grid faults) [6]-[8].

It has been reported that even though the WPP may be locally stable, this does not guarantee its large-signal stability, i.e. the ability to survive large grid impedance changes and large changes in WT reference currents [9]. Hence, there is a need to investigate the stability beyond the small-signal sense and develop rigorous analytical methods to map the system's stability boundary/ region of attraction (ROA). Where the ROA signifies a safe subset of the system's state space in which the trajectories converge to a stable equilibrium point [10]-[11].

This paper extends our ongoing research on non-linear system modelling and stability assessment for a wind turbine converter system [9],[12]. This paper reviews the performance of transient stability assessment methods such as the time-domain methods, i.e. time-domain simulations, and phase portrait analysis; and the analytical methods, i.e. equal-area criteria, and Lyapunov's direct method, for estimating the ROA of a post-disturbance WT converter system. Additionally, some highlights of advanced methods for transient stability assessment, such as the sum-of-squares optimisation technique and machine learning methods, are also presented.

The paper is organised as follows. Section II presents the equivalent swing equation model of a type-4 wind turbine suitable for large-signal stability analysis. Section III presents the review of the performance of transient stability assessment methods on the model described in section II. Finally, Section IV presents the conclusions of the work.

II. System Modelling

Owing to several advantages, type-4 wind turbines (WTs) with back-to-back converters have gained prominence for offshore wind power applications. For such turbine topologies, the action of the DC chopper is necessary under grid faults due to the power imbalance between the machine and grid side converters. Once the DC chopper is activated, the consequences are two-fold. Firstly, the DC voltage can be assumed to be steady. Secondly, the modelling of the machine-side converter can be ignored after the chopper is activated [13].

Furthermore, our earlier works [9],[12] discussed that the fast inner current control dynamics could be neglected when analysing the slow PLL dynamics for large-signal stability analysis. Also, it was shown that the impact of the shunt capacitor filter on the stability could be neglected if the current is controlled on the grid side LCL filter. The electrical model of the WT considered is presented in Fig. 1. Subsequently, a reduced-order representation of the WT in the DQ domain is illustrated in Fig. 2a. For synchronisation, a PLL with an synchronous rotation frame (SRF) approach (shown in Fig. 2b) is considered.

A. Equivalent swing equation of WT model

The SRF-PLL equation is given by [12]:

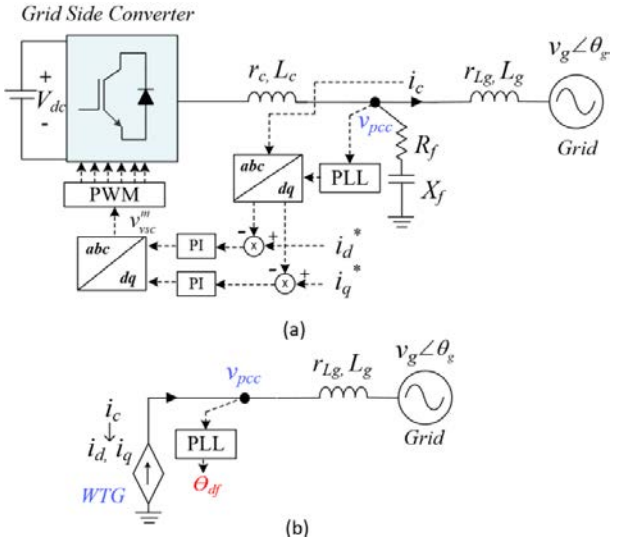

Fig. 1. (a) The electrical model of the type-4 WT with grid-side converter and controls. (b) The reduced-order electrical model of WT with assumptions considered in [9][12].

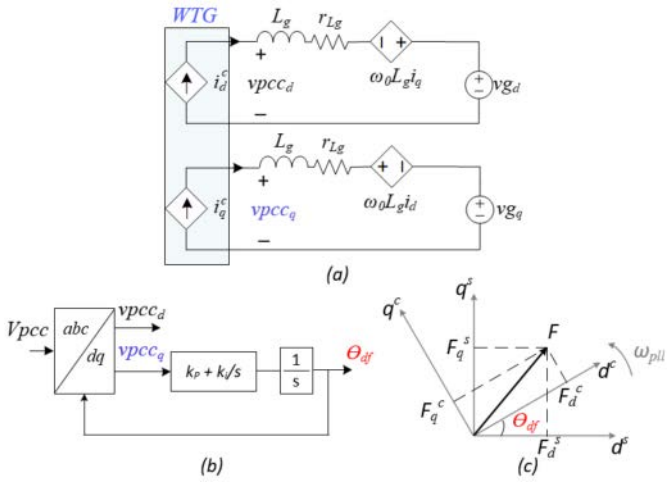

Fig. 2. (a) Reduced-order WT system representation in the DQ domain. (b) Typical synchronous reference frame PLL. (c) Vector diagram: Misalignment between the PLL reference frame and the grid reference frame.

$$\theta_{df} = \int \left(k_p vpcc_q^c + k_i \int vpcc_q^c dt \right) dt \tag{1}$$

$$\begin{aligned} vpcc_q^c = &-V_g \sin(\theta_{df} - \theta_g) + r_{Lg} i_q^c + L_g i_d^c \omega_g \\ &+ (\dot{\overline{L_g i_q^c}}) + L_g i_d^c (\dot{\overline{\theta_{df} - \theta_g}}) \end{aligned} \tag{2}$$

where, the gain k_p and k_i shape the dynamics of the SRF-PLL. θ_{df} and θ_g are the angle tracked by the PLL, and the grid voltage angle, respectively. i_d^c and i_q^c are the WT DQ currents in the PLL reference frame. The PLL reference frame and the grid reference frame rotate with the PLL frequency ω_{pll} and the actual grid frequency ω_g, respectively (as shown in Fig. 2c).

Equations (1) and (2) describe the transient nonlinear behaviour of the WT converter system. Given its second-order nature, it is possible to transform it into an equivalent swing equation and apply equivalent stability analysis. The equivalent swing equation of the WT converter system derived in [12] can be presented as,

$$M_{eq}\ddot{\delta} = T_{m_{eq}} - T_{e_{eq}} - D_{eq}\dot{\delta} \tag{3}$$

where,

$$\begin{aligned} M_{eq} &= 1 - k_p L_g i_d^c \\ T_{m_{eq}} &= k_p(\dot{\overline{r_{Lg} i_q^c}} + \ddot{\overline{L_g i_q^c}} + \dot{\overline{L_g i_d^c}}\omega_g) + k_i(r_{L_g} i_q^c \\ &\quad + \dot{\overline{L_g i_q^c}} + L_g i_d^c \omega_g) \\ T_{e_{eq}} &= (k_i V_g \sin\delta + k_p \dot{V}_g \sin\delta) + M_{eq}\dot{\omega}_g \\ D_{eq} &= k_p(V_g \cos\delta - \dot{\overline{L_g i_d^c}}) - k_i L_g i_d^c \end{aligned} \tag{4}$$

It should be noted that during the PLL synchronisation, i_d^c, i_q^c, V_g, and ω_g are not necessarily time-invariant, i.e. the post-fault active current recovers as a ramp function. The model described in (3) considers the time variance of the system parameters represented by the derivatives in (4); therefore, it is a non-linear non-autonomous damped differential equation. The accuracy of the equivalent swing equation of the WT was established in [12].

B. System Parameters

Table 1 presents the parameters describing the WT system considered in this study.

TABLE I
SYSTEM AND CONTROL PARAMETERS [14]

Symbol	Description	Value
S_b	Rated power	12 MVA
V_g	Nominal grid voltage (L-N, pk)	690 $\sqrt{2/3}$ V
f_g	Rated frequency	50 Hz
r_{Lg}, L_g	Grid-side impedance	SCR=2.3, X/R=17.2
i_d^c, i_q^c	Pre-disturbance active and reactive currents (pu)	1.0, -0.1
K_{pll}	SRF PLL design: k_p k_i	0.1, 30

The PLL gains are chosen to obtain an oscillatory PLL behavior.

C. Grid code requirements

As per grid code requirements [1]-[2], the WPPs are expected to stay connected during grid faults even when the grid voltage is very low, as seen in Fig 3b. During faults, reactive current injection is requested based on grid voltage dip, see Fig. 3a. For very low grid voltage the total reactive current magnitude is limited to 1pu. Subsequently, the active current is allowed to be decreased to keep the total current within the capability of the wind turbine.

III. Comparison Of Stability Assessment Methods

This section provides a review of various transient stability assessment methods. The primary objective of such an assessment is to determine whether the system will remain stable post a large disturbance. Such analysis plays a critical role in designing and/or evaluating the stability controls.

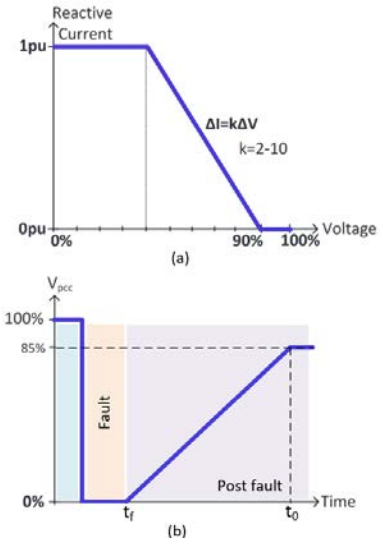

Fig. 3. Typical Grid code requirements: (a) Reactive current injection during grid faults; (b) Voltage profile during grid faults.

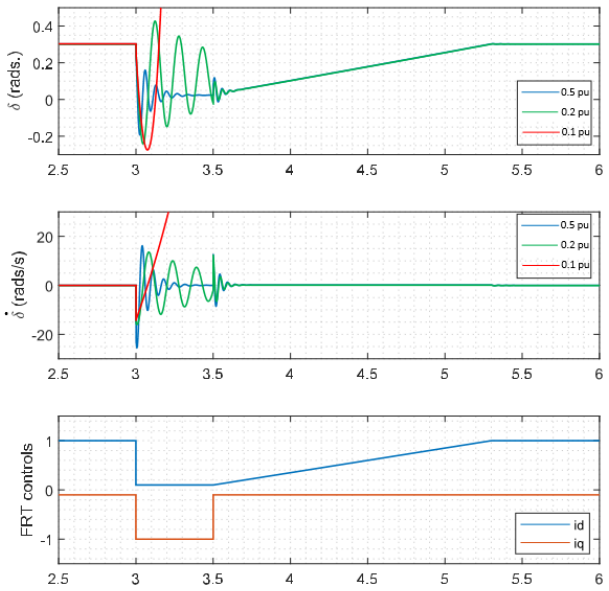

Fig. 4. Time-domain simulation: Three phase to ground grid fault with varying fault voltages.

A. Transient stability problem and objectives

Following a large disturbance, the system dynamics undergo a change once the disturbance is cleared. Figure 3b illustrates the stages during a disturbance, considering a three-phase bolted fault as an example. As seen in Fig. 3b, suppose the system has a stable post-disturbance equilibrium x_0=$\{\delta(t_0),\dot{\delta}(t_0)\}$, such that f($x_0$) = 0; then, as described in [15], the main problem of transient stability is if the system can reach x_0 from the post-fault initial condition x_f=$\{\delta(t_f),\dot{\delta}(t_f)\}$.

The enclosed area of the state-space that contains all the initial conditions x_f from which trajectories converge to x_0 is called the region of attraction (ROA). The ROA is denoted by A(x_0) and is defined as,

$$A(x_0) = \{x | \lim_{t\to\infty} \Phi(t,x) = x_0\} \tag{5}$$

Consequently, the objectives of transient stability assessment are:

- Identifying the post-disturbance initial condition x_f.
- Evaluating if x_f is within the ROA, if a post-disturbance stable equilibrium x_0 exists.
- Estimating the boundary of the ROA for the known x_0.

B. Time-Domain assessment methods

1) Time-domain simulation: Traditionally, transient stability has been assessed by running batches of time-domain simulations, where each simulation corresponds to a critical contingency at some operating point; then one needs to assess the results of each simulation to determine whether the response is stable.

A three-phase to ground fault with varying fault voltages is simulated to assess the transient stability of the system (3) defined by the parameters in Tab. 1. The fault is cleared after 500ms. As per grid code requirements, a fault ride-through control is implemented with a droop/k-factor of 2.5 (ref Fig. 3a). Post-fault active current recovers at the rate of 7.1 kA/s. The resulting trajectories are presented in Fig. 4.

From Fig. 4, it is observed that the system is stable for 0.5pu and 0.2 pu fault voltage, while the system goes unstable for a fault voltage of 0.1pu. In the time-domain simulation method, to investigate transient stability, the full disturbance needs to be simulated, i.e. pre-fault, fault and post-fault events. Moreover, the transient stability can only be observed for the predefined events simulated. As a result, this could result in missing out on critically stable events.

2) Phase portrait analysis: Phase portrait analysis is also a time domain simulation-based method. Second-order nonlinear differential equations that cannot be solved via analytical methods can be solved numerically and visualised graphically through phase portraits [16]. Instead of individually analysing time-domain simulations, one can use phase portraits to analyse a large amount of different initial conditions and visualise the trajectory of each solution in the phase plane.

For the system (3) defined by the parameters in Tab. 1, the post-fault initial conditions x_f are varied, and the subsequent unique trajectories are plotted in Fig. 5a. Additionally, the initial conditions x_f for which the trajectories converge to x_0 is plotted in Fig. 5b. Fig. 5b illustrates the post-fault system's ROA ($A_{PP}(x_0)$) in the state-space. From the initial condition marked with a blue dot, the system safely navigates to the stable equilibrium; however, from the red dot, it fails to converge because x_f is not contained within the ROA.

Geometrically, the ROA is a three-dimensional volume in the state-space since the post-fault active current in the system (3) also varies. Fig. 5b shows a slice of this volume in a two-dimensional plane corresponding to the PLL states. In Phase portrait method, only the post-disturbance trajectory needs to be simulated. The system will be stable as long as the post-disturbance initial condition is within the ROA.

Time-domain assessment methods are straightforward and do not need model simplification, i.e. non-autonomous model can be simulated without the need for complex mathematical algorithms. However, the limitation of such

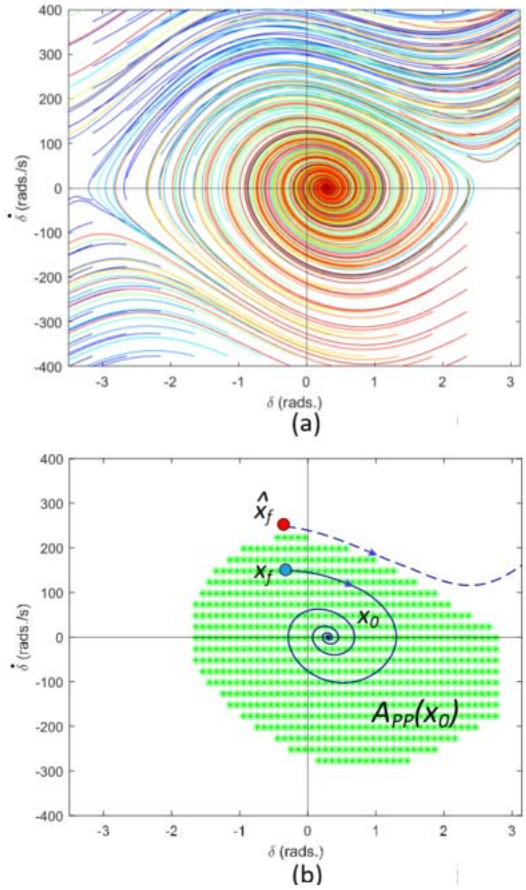

Fig. 5. (a) Phase portrait analysis of system (3); (b) A graphical illustration of the ROA. For the post-disturbance initial condition x_f, the system remains stable; however, for $\hat{x}_f$ it does not.

assessment methods are that they lacks a closed-form solution for quantifying the stability margins. To compensate for this limitation, repeated time-consuming simulations must be performed to identify the ROA. These factors highlight the need for analytical methods for quantifying the stability margins.

C. Analytical methods

Lyapunov's direct method is the main alternative to simulation-based stability assessment methods, and it provides a closed-form solution of a post-disturbance system.

Lyapunov's stability criteria: Assuming the post-disturbance system $f(x)$ has a stable equilibrium at x_0. Then the system is locally asymptotically stable in A(x_0) if a function $V(x)$ exists such that,

$$V(x) > 0, V(x_0) = 0, \dot{V}(x) = \nabla V(x) \cdot f(x) \leq 0 \qquad (6)$$

Analytically, it is difficult to obtain the exact ROA A(x_0). Instead, analytical methods try to find a relaxed set defined as,

$$A_\beta(x_0) = A(x_0) \cap \{x | V(x) \leq \beta \text{ and } \dot{V}(x) \leq 0\} \qquad (7)$$

where β is a positive constant that determines the boundary of $A_\beta(x_0)$ [17].

1) Equal Area criteria: The equal-area criterion (EAC) is a special case of Lyapunov's direct method [18] developed for power systems. Traditionally, EAC has been used for assessing transient stability of a two-machine or single-machine infinite bus system. EAC provides physical intuition about the swing equation i.e. the way synchronous generators (SG) respond to a disturbance. Since the EAC is widely applied for the transient stability analysis of SG, it is natural to extend it for the transient stability assessment of the system (3).

In EAC, it is customary to neglect the damping term. Fig. 6 shows an example of the power-angle characteristic of the WT, where the horizontal line indicates the mechanical torque T_m, and the sinusoidal curve represents electrical torque T_e. Post-fault, at steady state, the WT operates at the power angle δ_0. There also exists an unstable equilibrium point $\delta_{max} = \pi - \delta_0$. If the power angle exceeds δ_{max}, the WT goes out of step and the system becomes unstable [9].

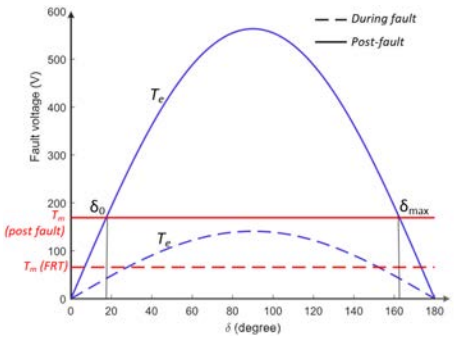

Fig. 6. Equal area criteria: post fault equilibrium points. Traditionally, for EAC the damping term is neglected.

The system (3) is a non-linear non-autonomous (time dependent) damped differential equation, however by simplifying the system to just a non-linear autonomous differential equation (i.e. ignoring the derivatives), a standard energy-function for a post-fault equilibrium point $x_0 = \{\delta_0, 0\}$ can be constructed as per (8) and (9).

$$\begin{aligned} V_{EAC}(x) &= M_{eq} \int_0^t x_2 \dot{x_2} dt - \int_0^t x_2 (T_{m_{eq}} - T_{e_{eq}}) dt \\ &= 0.5 M_{eq} x_{2,t}^2 - k_i V_g \left[\cos(x_{1,t}) - \cos(x_{1,0})\right] \\ &\quad - \left[k_i (R i_q^c + L_g i_d^c \omega_n)\right] (x_{1,t} - x_{1,0}) \\ &= KE(x_2) + PE(x_1) \end{aligned} \qquad (8)$$

$$\dot{V}_{EAC}(x) = -x_{2,t}^2 D_{eq} \implies 0 \text{ (damping neglected)} \qquad (9)$$

where, $x_1 = \delta$ and $x_2 = \dot{\delta}$. The contour plot for $V_{EAC}(x)$ is presented in Fig. 7. It may be observed that the energy is always positive except at the equilibrium point x_0 where it is zero. If the system is to remain stable following a disturbance, the energy of the disturbed system must not exceed a critical level $\beta = PE(\delta_{cr})$, as decribed in (7).

The technique for calculating $PE(\delta_{cr})$ is called the potential energy boundary surface (PEBS) method [19]. From Fig. 6, $\delta_{cr} = \delta_{max}$ for EAC. The region enclosed by $PE(\delta_{max})$ is the estimated ROA (red dotted) obtained from the EAC method, and is presented in Fig. 7.

Furthermore, in Fig. 8, a comparison of the ROA obtained from phase plane analysis and EAC is presented. It is

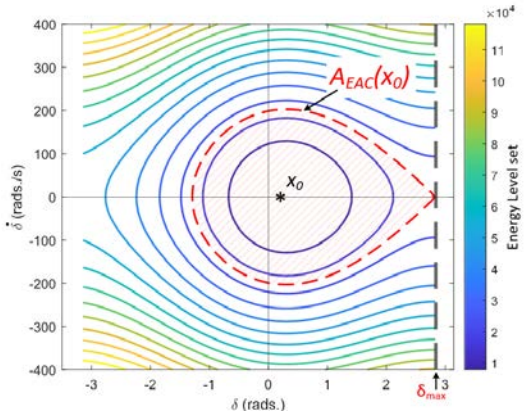

Fig. 7. Stability boundary proposed based on EAC.

observed that $A_{EAC}(x_0)$ is not fully a subset of $A_{PP}(x_0)$. There exists a state space in the first quadrant where the $A_{EAC}(x_0)$ is slightly optimistic when compared to the actual ROA $A_{PP}(x_0)$, i.e. for some initial conditions within $A_{EAC}(x_0)$, the system is unstable. This violates (7). The deviation can be accounted for by the neglected damping term in the EAC analysis.

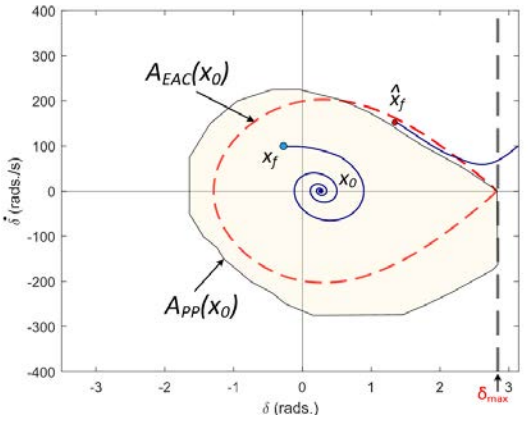

Fig. 8. Comparison of stability boundary: Phase plane vs EAC.

Unlike SGs, the damping coefficient D_{eq} in (3) is not a constant and cannot be ignored since it depends on the PLL angle δ and can be negative. Hence, for a better ROA estimation the damping term must be accounted for in the analysis.

2) Lyapunov's direct method: Here a general case of Lyapunov's direct method to access the transient stability is presented. Similar to EAC, considering the physical meaning of a SG, an energy-function for system (3), can be constructed as shown in (10) and (11). However, unlike EAC, the damping coefficient cannot be neglected, since D_{eq} is dependent on δ.

$$V_{LDM}(x) = 0.5M_{eq}x_{2,t}^2 - k_iV_g\left[\cos(x_{1,t}) - \cos(x_{1,0})\right] - \left[k_i(Ri_q^c + L_gi_d^c\omega_n)\right](x_{1,t} - x_{1,0}) \tag{10}$$

$$\dot{V}_{LDM}(x) = -x_{2,t}^2D_{eq} = -x_{2,t}^2[k_pV_g\cos(x_{1,t}) - k_iL_gi_d^c] \tag{11}$$

where, $x_1 = \delta$ and $x_2 = \dot{\delta}$. For $\dot{V}_{LDM}(x) \leq 0$, the dissipativity condition ($D_{eq} \geq 0$) has to be satisfied. The range (δ_{min}, δ_{max}) at which $D_{eq} \geq 0$ can be calculated as,

$$\delta_{D_{eq}=0} \Rightarrow \cos^{-1}[\frac{k_iL_gi_d^c}{k_pV_g}] \tag{12}$$

It must be noted that in (12), the derivatives in the damping term D_{eq} is neglected, since the energy function (10) was constructed assuming an autonomous behaviour of the system (3). For the system model (3) with parameters in Tab. 1, the contour plot $E_{LDM}(x)$ is illustrated in Fig. 9. The energy is always positive except at the equilibrium point x_0 where it is zero. However, $\dot{E}_{WT}(x) \leq 0$ is only guaranteed in the grey region. The estimated ROA for the system is the energy level set that touches critical level $+\delta_{D_{eq}=0}$, i.e. $\beta = PE(+\delta_{D_{eq}=0})$.

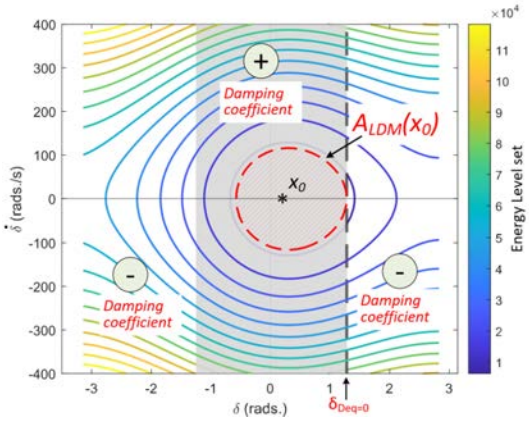

Fig. 9. Stability boundary proposed based on to positive damping.

In Fig. 10, a comparison of the ROA obtained from phase plane analysis, EAC and Lyapunov's direct method is presented. It is observed that $A_{LDM}(x_0)$ is a subset of $A_{PP}(x_0)$, satisfying (7). However, this method results in a conservative estimate of ROA. This conservatism can be accounted due to the strict constraint of positive damping. In reality, during transients the damping can be both positive and negative [20]. However, when the damping term becomes negative the proposed energy function (10) is not valid. Consequently, other approaches to obtain a valid energy function of the system (3) is needed which is less conservative or over optimistic.

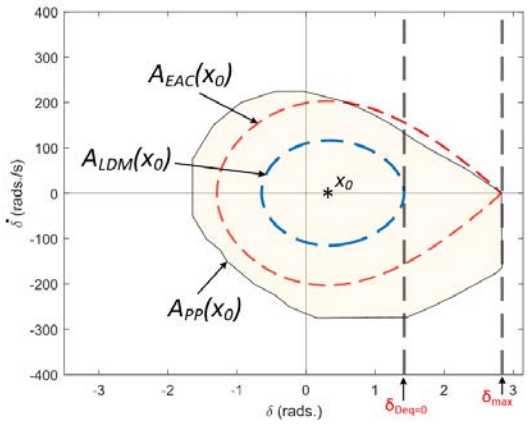

Fig. 10. Comparison of stability boundary: Phase plane vs EAC vs Lyapunov's direct method.

TABLE II
SUMMARY OF TRANSIENT STABILITY ASSESSMENT METHODS

Transient stability methods	Computation burden	Method Complexity	System Dynamics		Region of attraction
			Damping term	Post fault active current ramp	
Time-domain simulation	Though predefined events are simulated, the full disturbance needs to be simulated, i.e. pre-fault,fault and post-fault events.	Straightforward and do not require complex mathematical algorithms. Needs power system expertise.	Yes	Post fault current ramp rate is considered (i.e non-autonomous model).	No
Phase portrait analysis	Repeated time-consuming, post-fault simulations have to be performed to identify the ROA.	Straightforward and do not require complex mathematical algorithms. Needs power system expertise.	Yes	Post fault current ramp rate is considered (i.e. non-autonomous model).	Provides exact ROA.
Equal area criteria	Very low computation burden needed since closed form solution exists.	Obtaining closed form solution is complex. Readily understood in terms of physics of the system.	Usually neglected in EAC.	Ramp rate is neglected (i.e. autonomous model). To consider ramp rate, energy functions for non-autonomous systems needs to be investigated.	Based on assumptions it estimates slightly optimistic ROA.
Lyapunov's direct method	Very low computation burden needed, since closed form solution exists.	Obtaining closed form solution is complex. Readily understood in terms of physics of the system.	Yes	Ramp rate is neglected (i.e. autonomous model). To consider ramp rate, energy functions for non-autonomous systems needs to be investigated.	Based on assumptions it estimates highly conservative ROA.
Sum-of-squares optimisation	Computation burden depends upon the optimisation problem, however less than time domain methods.	High complexity, since the system and energy function needs to be converted to poly-nomials, and then the SOS problem has to be converted to SDP.	Yes	As per literature, most SOS problems has been carried out for autonomous models. To include ramp rate further investigation is needed.	Provides ROA where its boundary is a maximisation problem. Can be larger than Lyapunov's direct method.
Machine learning methods	High computation burden, since ML model has to be trained over large volumes of data.	Complexity depends on the type of ML algorithm chosen. Needs power systems and ML expertise. ML does not provide an intuitive physical interpretation of system behaviuor.	Yes	Post fault current ramp rate can be easily considered since analysis depends on training data (i.e. non-autonomous model can be trained).	Depends upon the ML technique chosen, can estimate ROA closer to Phase portrait analysis.

3) Sum-of-squares optimisation: The energy function approach based on sum-of-squares (SOS) optimisation has recently attracted attention [21]–[24]. Here, the Lyapunov function and ROA estimates are formulated as an optimisation problem, achieved by inserting the stability criteria (6) into the objective function and its constraints. SOS optimisation requires that the post-fault system *f(x)* must be polynomial in the state variables [21]. For $x \in R^n$, the polynomial $p(x)$ is said to be a SOS if there exist polynomials $\{q_i\}_{i\in I}$ such that,

$$p(x) = \sum_{i\in I} q_i^2(x) \geq 0 \tag{13}$$

Hence, once the post-fault system *f(x)* and corresponding Lyapunov function *V(x)* is expressed as polynomials [24], then the stability criteria (6) can be formulated as an SOS optimisation problem [21] as,

$$\begin{aligned} \underset{\beta,s,V}{\text{Maximise}} \quad & \beta \\ \text{subject to} \quad & -\nabla V(x)\cdot f(x) + s(x)[V(x)-\beta] \\ & V(0) = 0, \end{aligned} \tag{14}$$

where, the dummy polynomial $s(x)$ is formulated using the S-procedure [22]. To solve the SOS optimisation problem (14), it is restructured as a semidefinite program (SDP). The MATLAB toolboxes such as SOSOPT and SOSTOOLS enable the translation from SOS problem to SDP [25-26]. The contour plot of $V(x) \leq \beta$, similar to (7), gives the optimised ROA. The ROA obtained could be larger than that of Lyapunov's direct method. As per literature, most SOS transient stability problems has been carried out without considering a ramp rate change (i.e. autonomous models are used). To include the post fault current ramp rate in the optimisation problem, further investigation is needed.

The SOS method provides an organised approach to building the Lyapunov function and obtaining an optimised ROA. The methodology does not force any modelling limitations, except that the post-fault system model must be expressed through a polynomial function. A known challenge of the SOS approach is that as the order of the energy function or the states of the system increases, the computational complexity of the SDP problem increases, wherein the optimisation can fail or at times lead to flawed solutions.

D. Machine learning methods

Various machine learning (ML) methods have been studied for transient stability analysis, including decision trees and neural networks [27]-[29]. ML-based stability assessment methods require building a predictive model using data from measurements. The model is then trained to find a function that maps the inputs, e.g., fault voltage, and the output, i.e. stable/unstable classification. ML models requires large volumes of data, and collecting this data with the required resolution is not always possible. Hence, training data is often augmented with data from time-domain simulations.

ML-based transient stability assessment is well suited for systems with complex and diverse control systems. For example, the analytical methods, the energy function constructed did not consider time-varying ramp rate current controls; however, ML-based approach has no such limitation. However, training the ML models is highly heuristic. Also, they do not present an intuitive physical interpretation of the system's behaviour.

E. Summary of transient stability assessment methods

A summary of transient stability assessment methods is presented in Tab. II. The important features that bring out the difference among the stability assessment methods are only listed. In general, the time-domain methods are less complex and provides accurate ROA, accompanied by a high computation burden. On the other hand, the analytical methods are complex and provides either slightly optimistic (for equal area criteria) or highly conservative (for Lyapunov's direct method) estimates of the ROA; however, such methods are very fast due to closed-form solutions.

IV. Conclusions

This paper reviews the performance of transient stability assessment methods such as the time-domain methods, i.e. time-domain simulations, and phase portrait analysis; and the analytical methods, i.e. equal-area criteria, and Lyapunov's direct method, for estimating the region of attraction (ROA) of a post-disturbance WT converter system. Additionally, some highlights of advanced methods for transient stability assessment, such as the sum-of-squares optimisation technique and machine learning methods, are also presented. The following was concluded:

1) Time-domain assessment methods, such as time domain simulation and phase portraits are straightforward and do not need model simplification, i.e. non-autonomous model can be simulated without the need for complex mathematical algorithms. A limitation of time-domain methods are that they lacks a closed-form solution for quantifying the stability margins; to compensate for this limitation, repeated time-consuming simulations must be performed to identify the ROA.
2) The merits of analytical methods, such as equal area criteria, Lyapunov's direct method, and SOS optimisation are that they have clear physical meaning and could give an analytical estimation of stability boundaries - ROA. However, the existing approach to construct energy functions has assumptions (i.e. autonomous system) leading to either slightly optimistic (for equal area criteria) or highly conservative (for Lyapunov's direct method) estimates of the ROA.
3) ML-based approaches have no limitation with regards to implementing converter controls (i.e. non-autonomous system). That said, training ML models is highly heuristic. Also, ML models do not present an intuitive physical interpretation of the system's behaviour.

References

[1] "Technical regulation 3.2.5 for wind power plants above 11 kW", Energinet 13/96336-43.

[2] "Offshore-Netzanschlussregeln (O-NAR)", Tech. rep. TenneT TSO GmbH, August 2019.

[3] "The Grid Code - Issue 6 Revision 12", Tech. rep. National Grid, March 2022.

[4] D. Wang, J. L. Rueda Torres, A. Perilla, E. Rakhshani, P. Palensky and M. A. A. M. van der Meijden, "Enhancement of Transient Stability in Power Systems with High Penetration Level of Wind Power Plants," 2019 IEEE Milan PowerTech, 2019, pp. 1-6. [2]

[5] Y. Li et al., "PLL Synchronization Stability Analysis of MMC-Connected Wind Farms Under High-Impedance AC Faults," in IEEE Transactions on Power Systems, vol. 36, no. 3, pp. 2251-2261.

[6] Göksu, Ö., S, P., Iov, F. , Bak, C. L. , Teodorescu, R., Kjær, P.C., "Loss of Synchronism of Wind Turbine Converters during Low Voltage Grid Faults". Proceedings of the 13th International Workshop on Large-Scale Integration of Wind Power into Power Systems as well as on Transmission Networks for Offshore Wind Power Plants (WIW2014) Energynautics.

[7] I. Erlich, F. Shewarega, S. Engelhardt, J. Kretschmann, J. Fortmann and F. Koch, "Effect of wind turbine output current during faults on grid voltage and the transient stability of wind parks," 2009 IEEE Power Energy Society General Meeting, 2009, pp. 1-8.

[8] S. Ma, H. Geng, L. Liu, G. Yang and B. C. Pal, "Grid-Synchronisation Stability Improvement of Large Scale Wind Farm During Severe Grid Fault," in IEEE Transactions on Power Systems, vol. 33, no. 1, pp. 216-226, Jan. 2018.

[9] S. Ghosh, G. Yang, M. K. B. Dowlatabadi and L. Kocewiak, "Nonlinear stability analysis of a reduced-order wind turbine VSC-grid model operating in weak grid conditions," 20th International Workshop on Large-Scale Integration of Wind Power into Power Systems as well as on Transmission Networks for Offshore Wind Power Plants (WIW 2021), 2021, pp. 457-463.

[10] S. L. Brunton, B. W. Brunton, J. L. Proctor, and J. N. Kutz, "Koopman invariant subspaces and finite linear representations of nonlinear dynamical systems for control,"PLOS ONE, vol. 11, no. 2, pp. 1–19, Feb. 2016.

[11] Y. Li, H. He, J. Wu, D. Katabi, and A. Torralba, "Learning compositional koopman operators for model-based control," inProc. Intl. Conf. Learning Represent., 2020

[12] Mohammad Kazem Bakhshizadeh, Sujay Ghosh, Łukasz Kocewiak, and Guangya Yang. (2022). Improved Reduced-Order Model for PLL Instability Investigations. https://doi.org/10.5281/zenodo.7016303

[13] Chen Zhang, Xu Cai, Atle Rygg, Marta Molinas, Modeling and analysis of grid-synchronizing stability of a Type-IV wind turbine under grid faults, International Journal of Electrical Power Energy Systems, Volume 117, 2020,

[14] Ł. Kocewiak, R. Blasco-Giménez, C. Buchhagen, J. B. Kwon, Y. Sun, A. Schwanka Trevisan, M. Larsson, X. Wang, "Overview, Status and Outline of Stability Analysis in Converter-based Power Systems," The 19th International Workshop on Large-Scale Integration of Wind Power into Power Systems. as well as Transmission Networks for Offshore Wind Farms, Energynautics GmbH, 11-12 November 2020.

[15] P. Varaiya, F. F. Wu, and R. Chen, "Direct methods for transient stability analysis of power systems: Recent results,"Proc. IEEE, vol. 73, no. 12, pp. 1703–1715, Dec. 1985

[16] Y. A. Kuznetsov, Ch-1. Introduction to Dynamical Systems, "Elements of applied bifurcation theory", 2nd edition, Springer.

[17] H. Choi, P. J. Seiler, and S. V. Dhople, "Robust power systems stability assessment with sum of squares optimization," inProc. IEEE Power Energy Soc. Gen. Meeting, 2015, pp. 1–5.

[18] R. H. Park and E. H. Bancker, "System stability as a design problem," Trans. AIEE, vol. 48, no. 1, pp. 170–193, Jan. 1929.

[19] Y. Xu, Z. Y. Dong, J. Zhao, Y. Xue, and D. J. Hill, "Trajectory sensitivity analysis on the equivalent one-machine-infinite-bus of multi-machine systems for preventive transient stability control,"IET Gener. Transm. Distrib., vol. 9, no. 3, pp. 276–286, 2015.
[20] Y. Lu, Z. Du, Y. Li and Y. Zhang, "Nonlinear Damping Property and Limit Cycle of VSC," in IEEE Transactions on Power Delivery, 2022, doi: 10.1109/TPWRD.2022.3181852.
[21] S. Izumi, H. Somekawa, X. Xin, and T. Yamasaki, "Estimation of regions of attraction of power systems by using sum of squares programming," Electr. Eng., vol. 100, no. 4, pp. 2205–2216, Dec. 2018.
[22] P. A. Parrilo, "Structured semidefinite programs and semialgebraic geometry methods in robustness and optimization," Doctoral dissertation, California Institute of Technology, 2000.
[23] W. Tan and A. Packard, "Stability region analysis using polynomial and composite polynomial Lyapunov functions and sum-of-squares programming,"IEEE Trans. Autom. Control, vol. 53, no. 2, pp. 565–571, 2008.
[24] Zhang C, Molinas M, Li Z and Cai X (2020) Synchronizing Stability Analysis and Region of Attraction Estimation of Grid-Feeding VSCs Using Sum-of-Squares Programming. Front. Energy Res. 8:56.
[25] P. Seiler, "SOSOPT: A toolbox for polynomial optimization," 2013.
[26] S. Prajna, A. Papachristodoulou, and P. Parrilo, "Introducing SOSTOOLS: A general purpose sum of squares programming solver," inProc. IEEE Conf. Decision and Control, vol. 1, 2002, pp. 741–746.
[27] B. Wang, B. Fang, Y. Wang, H. Liu, and Y. Liu, "Power system transient stability assessment based on big data and the core vector machine,"IEEE Trans. Smart Grid, vol. 7, no. 5, pp. 2561–2570, 2016.
[28] O. A. Alimi, K. Ouahada, and A. M. Abu-Mahfouz, "A review of machine learning approaches to power system security and stability,"IEEE Access, vol. 8, pp. 113 512–113 531, 2020.
[29] S. You, Y. Zhao, M. Mandich, Y. Cui, H. Li, H. Xiao, S. Fabus, Y. Su, Y. Liu, H. Yuan, H. Jiang, J. Tan, and Y. Zhang, "A review on artificial intelligence for grid stability assessment," inProc. IEEE Int. Conf. on Commun. Control and Comput. Technol. for Smart Grids, 2020, pp. 1–6.